

Chapter 3

Simulations of tides in the Mandovi and Zuari estuaries

3.1 Introduction

In this chapter, the simulations of tides, tidal currents, freshwater influence on tides and the studies on tidal asymmetries are described. Tidal estuaries serve as vital components to coastal ecosystems throughout the world. They usually have complex geometry and strongly nonlinear tidal dynamics [McLaughlin et al., 2003]. As mentioned previously, tide is the main driving mechanism in the estuaries. The Mandovi and Zuari estuaries are meso-tidal estuaries where tidal range is about 1.5 and 2.3 *m* during neap and spring tides respectively. The numerical model, boundary conditions used for the simulations and the results are described in the following sections.

3.1.1 Numerical model

The hybrid network numerical model described in Chapter 2 was used for the simulations of tidal amplitude, tidal currents etc. in the Mandovi, Zuari and Cumbarjua canal. Sim-

ulations of tidal currents were carried out in the 2D domain of the Mandovi and Zuari estuaries. The details of the equations and numerical scheme used in the model have been explained in Chapter 2.

3.1.2 Initial and boundary conditions

Tide, for forcing the model at the open boundary was predicted from the known tidal constituents at Mormugao (Figure 1.2) using Tidal Analysis Software Kit-2000. At the western boundary (open boundary) of the model, surface elevation was defined as a function of time, while zero flux conditions were applied in the eastern, southern and northern boundaries. The model was initialised with zero surface elevation and velocity throughout the network. At the upstream end of the model domain, transport was calculated from the available river discharge rate.

3.1.3 The coefficients used in the model

The coefficient of horizontal diffusion of momentum, A_H , was chosen to be $500 \text{ m}^2\text{s}^{-1}$ in the present model. There was no considerable variation in amplitude at different stations in the estuaries when the bottom drag coefficient, C_D , in the model was allowed to vary from 0.001 to 0.003, however, the value of 0.002 showed better agreement between observed and simulated tides. Hence we used 0.002 as a constant value for bottom drag coefficient in the downstream regions of the model. At the upstream regions, the channels bathymetry plays an important role on tides. So the Manning coefficient in 1D model was allowed to vary from 0.015 to 0.035.

3.2 Results

To simulate tides, the model was run for different cases. First, for the simulation of longitudinal variation of tides during dry and wet seasons and influence of river discharge

on tides. Second, for the simulation of tidal currents and third, for the simulation of tidal constituents. The details of the simulations and the results are described in the following sections.

For simulation of tides, the hybrid network model with initial and boundary conditions was run for 6 days each for dry and wet seasons. The model was forced with sea surface elevation at the open boundary as described previously. During wet season, the Mandovi and Zuari estuaries receive huge amount of fresh water. Figure 1.5 shows the discharge at Ganjem in 1993. The river discharge was about $400 \text{ m}^3 \text{ s}^{-1}$ during July and August (Bars correspond to 7 and 8 along the x-axis). Hence, river discharge of $400 \text{ m}^3 \text{ s}^{-1}$ was introduced at upstream end of the model domain. The model was run for 6 days (12 tidal cycles). The first 3 days were considered for spin-up and the remaining 3 days simulations were used for the comparison with the observations.

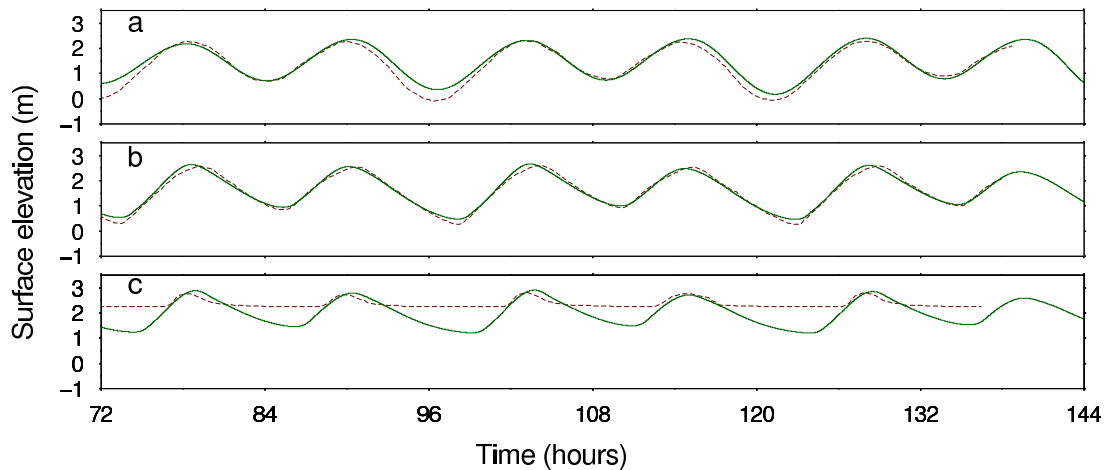
3.2.1 Simulations of tides in the Mandovi estuary

Figure 3.1 shows the simulated tides during dry season in the Mandovi estuary. There is a good agreement between the simulations and observations at Mormugao (Figure 3.1 a) and Volvoi (Figure 3.1 b) and at Ganjem (Figure 3.1 c), the simulations are reasonably good. What is noticed from the Figure 3.1 is that, when tide reaches at Ganjem, tidal range is reduced to less than 0.5 m from 2.1 m . The simulations of tide during wet season are also reasonably well in the Mandovi (Figure 3.3). The presence of tidal oscillations is negligible at Ganjem during wet season.

3.2.2 Simulations of tides in the Zuari estuary and Cumbarjua canal

Observed and simulated tides during dry and wet seasons in the Zuari estuary and Cumbarjua canal are shown in Figures 3.3 and 3.4 respectively. The model could simulate the observed tides well in both dry and wet seasons in the Zuari estuary. The magnitude of

Figure 3.1 Observed (dotted line) and simulated (solid line) tides at different stations in the Mandovi estuary in April 1993. The panels a, b and c represent Mormugao, Volvoi and Ganjem respectively. 72 *hours* shown on the x-axis correspond to 0.0 *hours* (IST) on 07/04/1993.



the tidal amplitude at Banastarim in the Cumbarjua canal (Figures 3.3 b and 3.4 b) are almost equal to that of Zuari. This shows that tide is propagated to the Cumbarjua canal from Zuari without any dissipation in amplitudes. At Sanguem, an upstream end station in the Zuari estuary (Figures 3.3 c), tidal amplitude during dry season is not reduced as in the case of Ganjem in the Mandovi.

3.2.3 Simulations of tidal currents

Tidal observations carried out during April and August 1993 were used for the validation of model. The simulations of tides were reasonably well in these estuaries and the simulation of tide showed that the model could be used for the simulation of tidal currents in these estuaries. For the simulation of tidal currents, the model was run for 1 month and the simulations were carried out during the spring and neap tides in April 1993. The purpose of running the model in the month of April was to determine the tidal currents in the absence of river discharge. To simulate tidal currents, the model was forced at open

Figure 3.2 Observed (dotted line) and simulated (solid line) tides at different stations in the Mandovi estuary in August 1993. The panels a, b and c represent Mormugao, Volvoi and Ganjem respectively. 72 hours shown on the x-axis correspond to 0.0 hours (IST) on 19/08/1993.

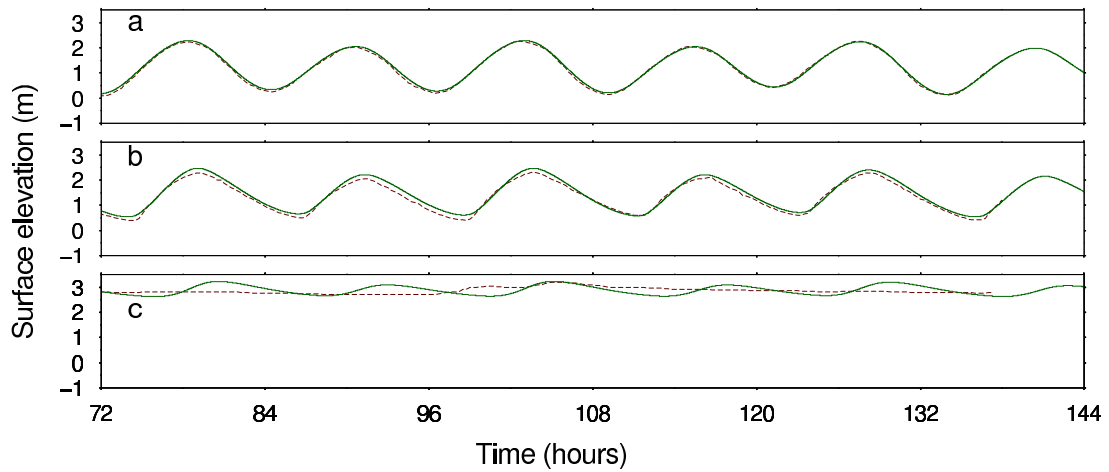


Figure 3.3 Observed (dotted line) and simulated (solid line) tides at different stations in the Zuari estuary and Cumbarjua canal in April 1993. The panels a, b and c represent Mormugao, Banastarim and Sanguem respectively. 72 hours shown on the x-axis correspond to 0.0 hours (IST) on 07/04/1993.

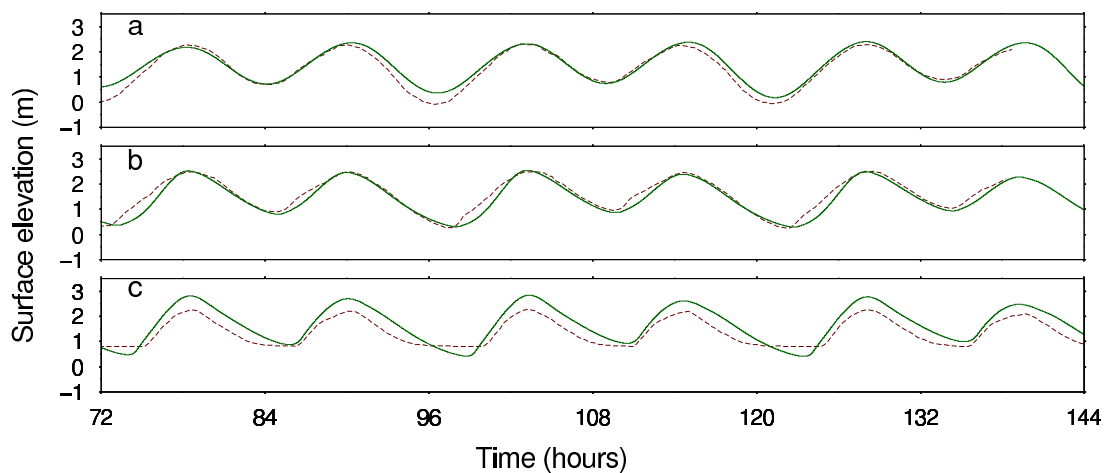
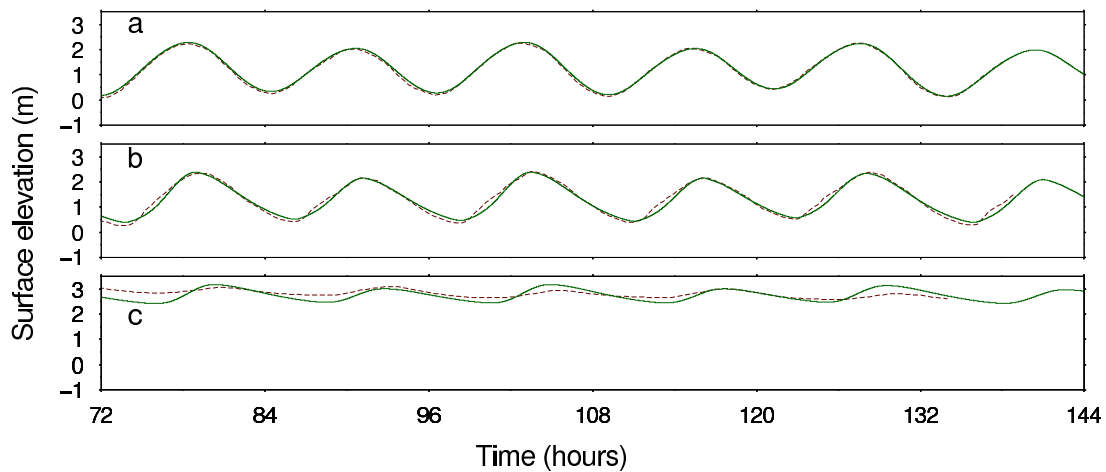


Figure 3.4 Observed (dotted line) and simulated (solid line) tides at different stations in the Zuari estuary and Cumbarjua canal in August 1993. The panels a, b and c represent Mormugao, Banastarim and Sanguem respectively. 72 hours shown on the x-axis correspond to 0.0 hours (IST) on 19/08/1993.



boundary with sea surface elevation as a function of time.

Tidal ranges in both the Mandovi and Zuari estuaries are about 2.3 and 1.5 m during spring and neap tides respectively. Tidal currents simulated for spring tide are shown in Figures 3.5–3.7. Fairly strong tidal currents of about 0.80 m s^{-1} were found during this period in the downstream regions of these estuaries. The magnitude of tidal currents are reduced to about 0.4 m s^{-1} during the neap tide (Figure 3.8–3.10). The magnitude of tidal currents are high in the Zuari than compared to Mandovi. This is because of the higher depth in the Zuari compared to Mandovi. Tidal current observations [DeSousa, 1999a, 2000], at Campal, near the mouth of the Mandovi estuary were carried out on 15–16 April 1999. These measurements of tidal currents show that the magnitude of tidal currents is of about 1.0 m s^{-1} during spring tide whereas the observations during neap tide (12–13 February 2000) show that the magnitude of these currents are of about 0.65 m s^{-1} . The simulated currents are slightly lower than that of those observed.

To study the tidal currents during wet season, the tidally averaged currents over a M_2

Figure 3.5 Tidal currents during the spring tide in the Mandovi and Zuari estuaries. The currents shown are only for the 2D domain of the 1D and 2D model domain. The sea surface elevation predicted for April 1993 at Mormugao was used for prescribing boundary condition at the open boundary. The timings shown are with respect to the occurrence of high tide at Mormugao.

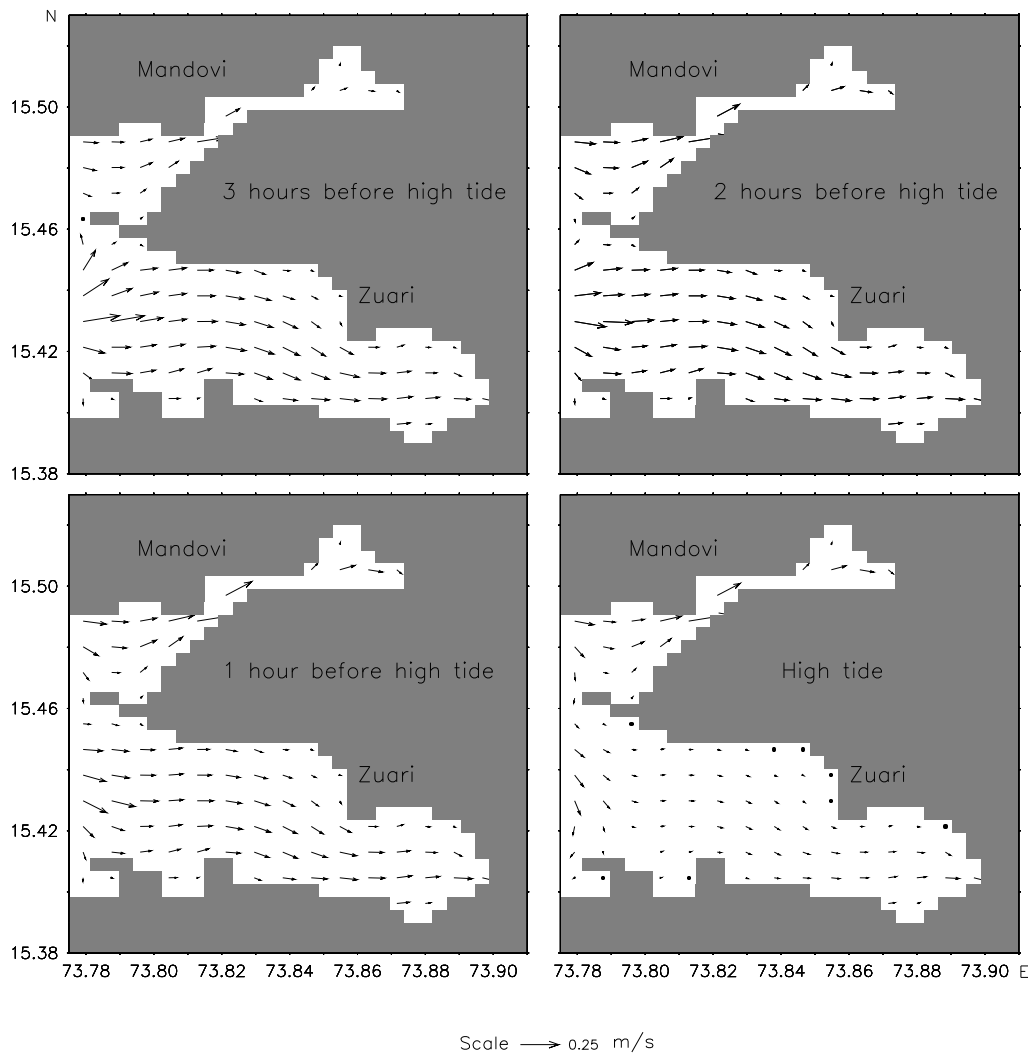


Figure 3.6 (Continued) Tidal currents during the spring tide in the Mandovi and Zuari estuaries. The currents shown are only for the 2D domain of the 1D and 2D model domain. The sea surface elevation predicted for April 1993 at Mormugao was used for prescribing boundary condition at the open boundary. The timings shown are with respect to the occurrence of high tide at Mormugao.

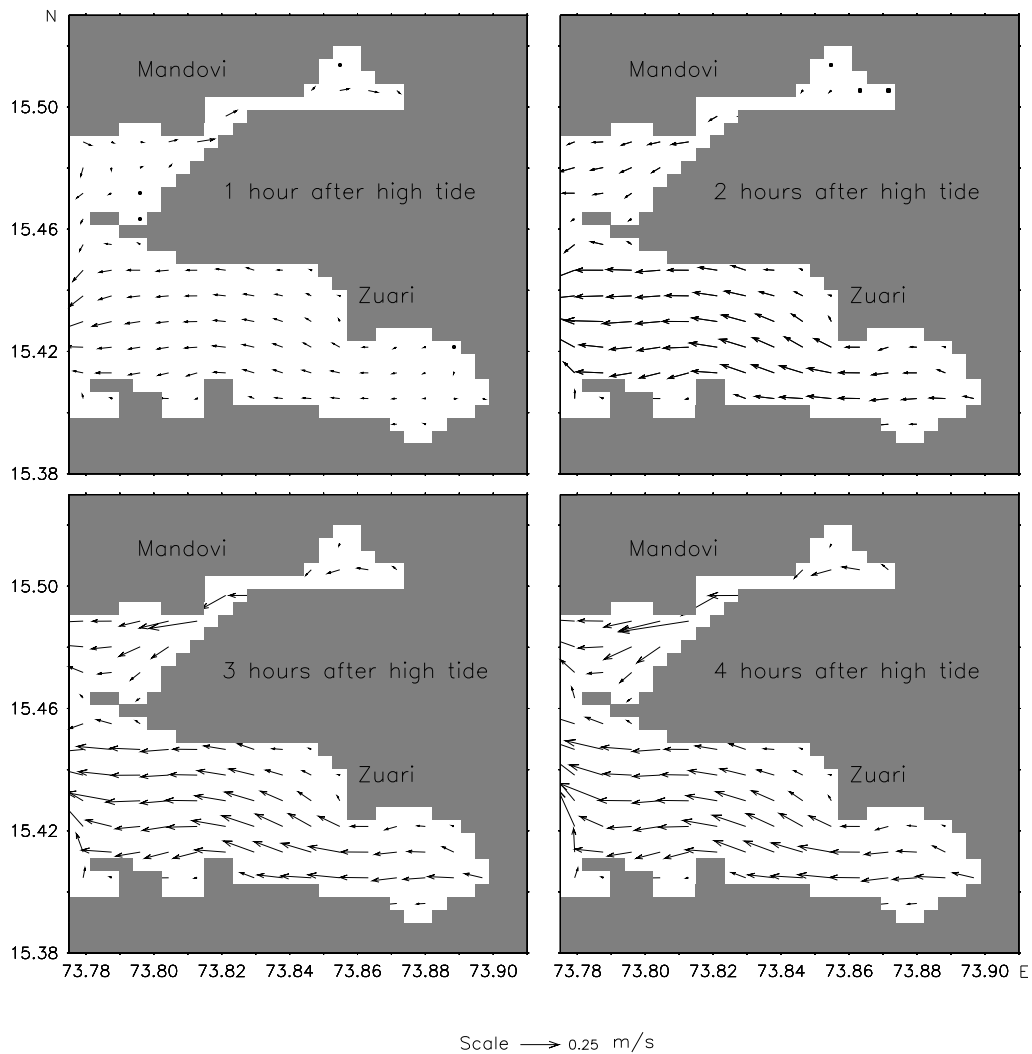


Figure 3.7 (Continued) Tidal currents during the spring tide in the Mandovi and Zuari estuaries. The currents shown are only for the 2D domain of the 1D and 2D model domain. The sea surface elevation predicted for April 1993 at Mormugao was used for prescribing boundary condition at the open boundary. The timings shown are with respect to the occurrence of high tide at Mormugao.

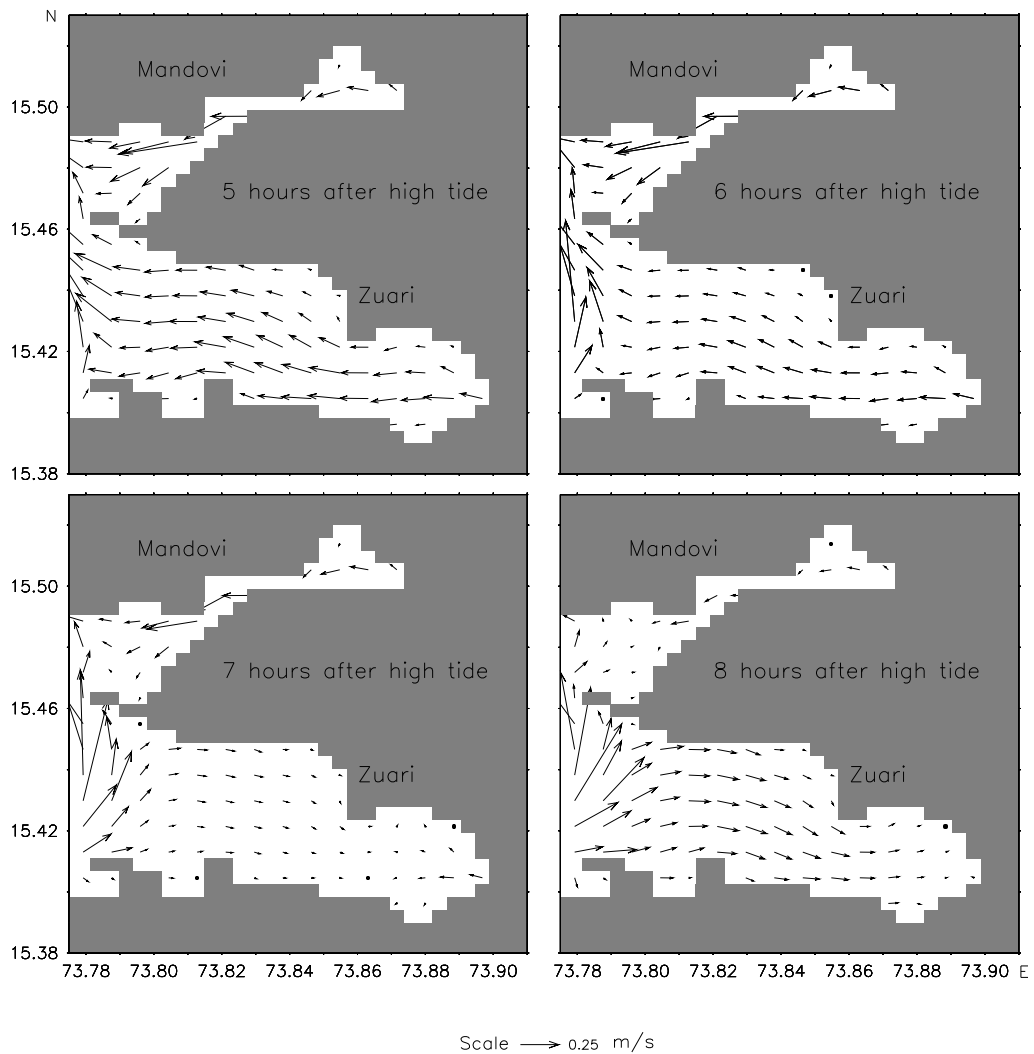


Figure 3.8 Tidal currents during the neap tide in the Mandovi and Zuari estuaries. The currents shown are only for the 2D domain of the 1D and 2D model domain. The sea surface elevation predicted for April 1993 at Mormugao was used for prescribing boundary condition at the open boundary. The timings shown are with respect to the occurrence of high tide at Mormugao.

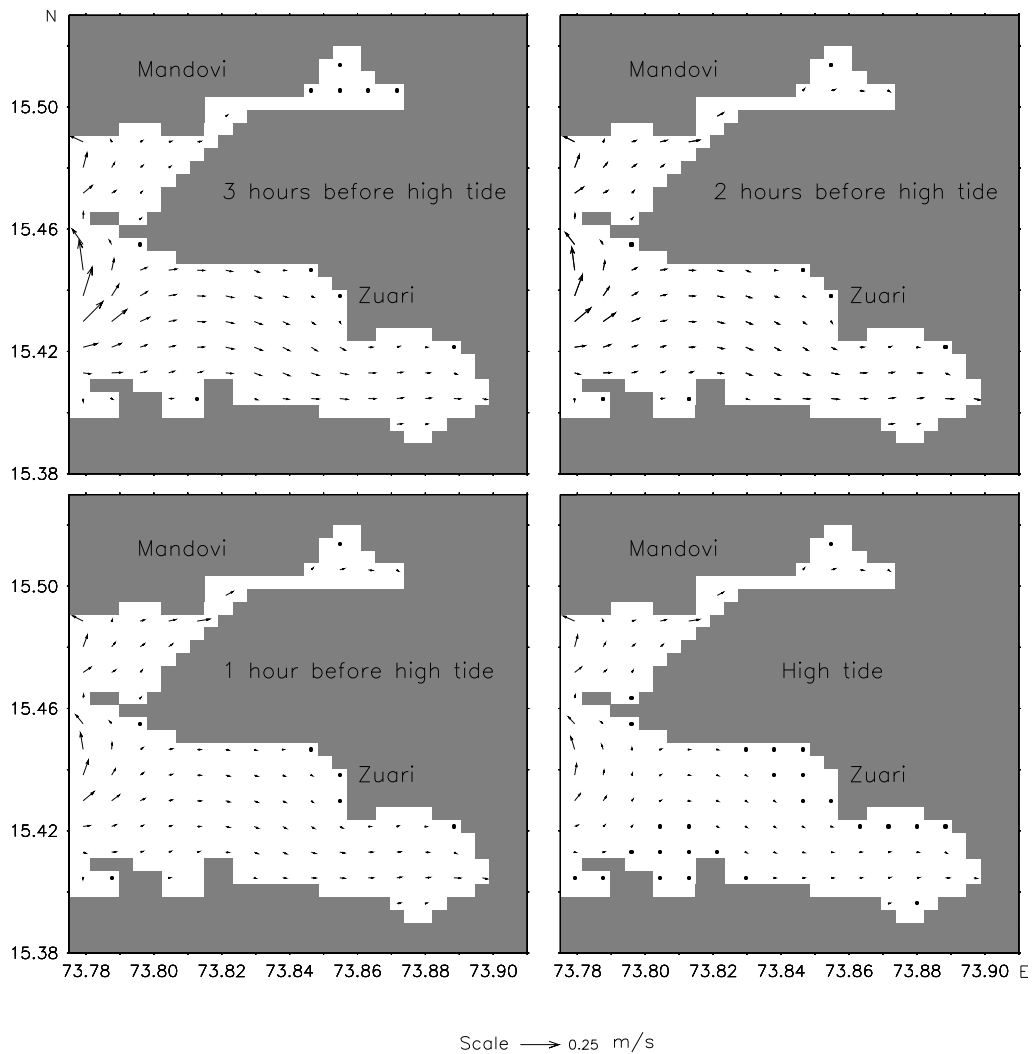


Figure 3.9 (Continued) Tidal currents during the neap tide in the Mandovi and Zuari estuaries. The currents shown are only for the 2D domain of the 1D and 2D model domain. The sea surface elevation predicted for April 1993 at Mormugao was used for prescribing boundary condition at the open boundary. The timings shown are with respect to the occurrence of high tide at Mormugao.

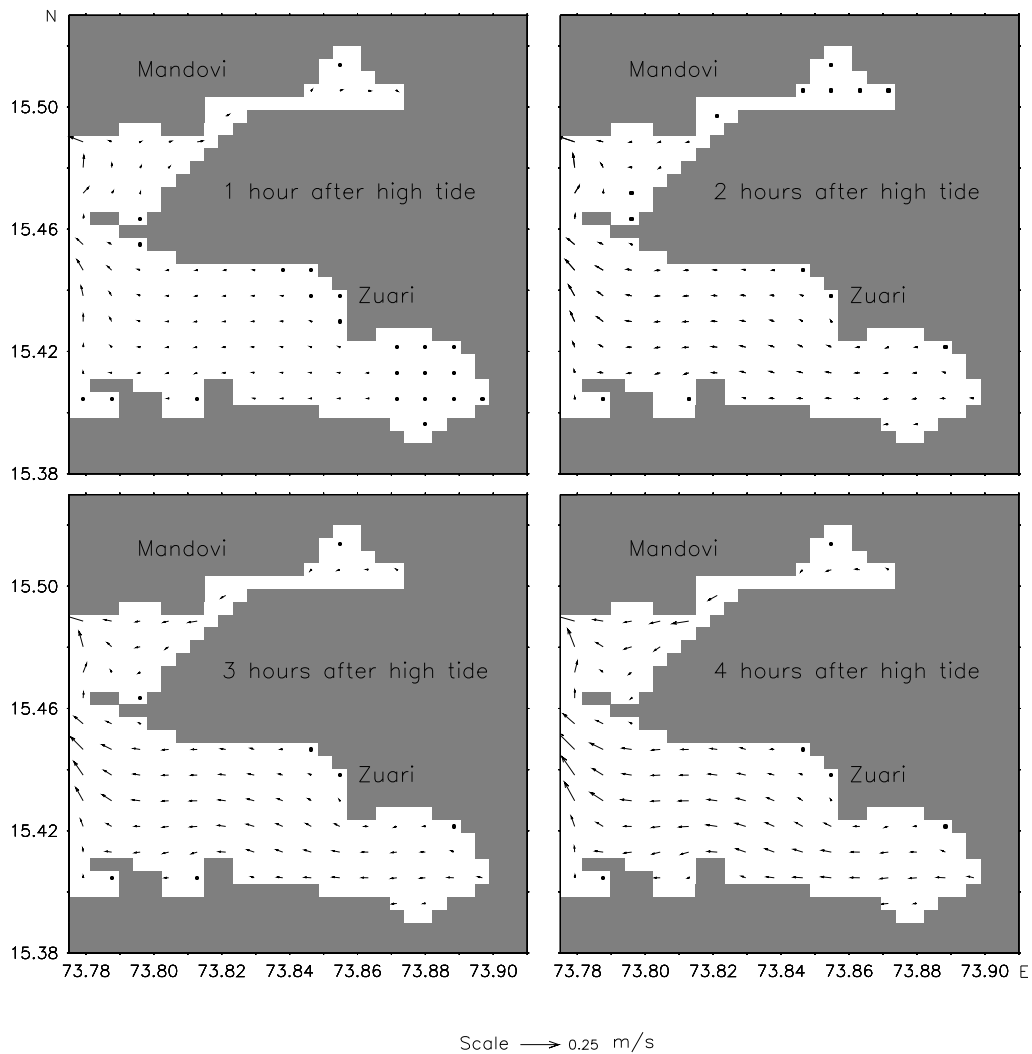
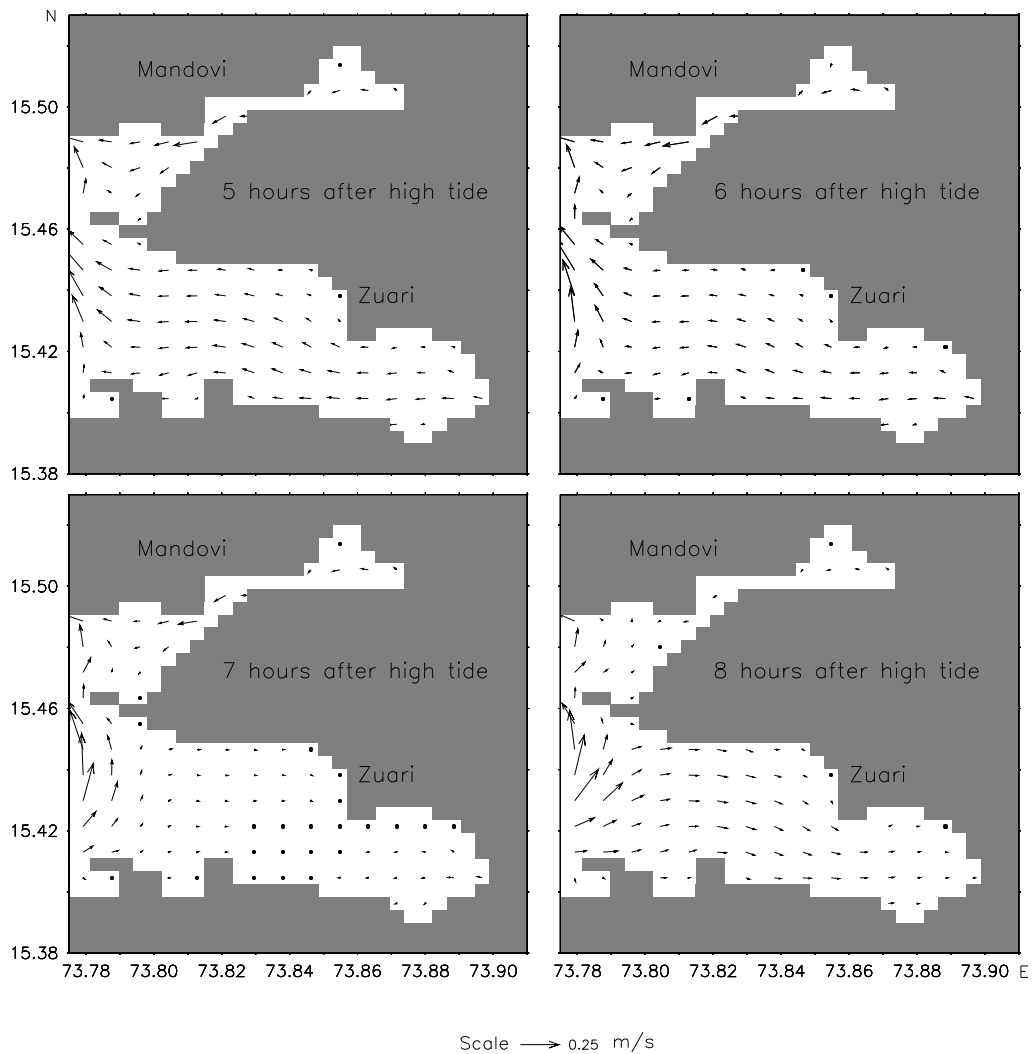


Figure 3.10 (Continued) Tidal currents during the neap tide in the Mandovi and Zuari estuaries. The currents shown are only for the 2D domain of the 1D and 2D model domain. The sea surface elevation predicted for April 1993 at Mormugao was used for prescribing boundary condition at the open boundary. The timings shown are with respect to the occurrence of high tide at Mormugao.



tidal period was calculated for varying river discharges. The details of the simulations residual currents and flushing time are explained in Chapter 4 of this thesis.

3.3 Tidal asymmetry

One of the main objectives of this thesis was to study the tidal asymmetries in the Mandovi and Zuari estuaries. Tidal spectrum consists of large number of constituents and amplitude and phase of these constituents are subjected to distortion when they propagate from ocean to estuaries. Bottom friction, channel geometry and other physical processes cause tidal distortion in an estuary. Tidal asymmetry has important effects on both the geological evolution of shallow estuaries and the navigability of estuarine channels [Aubrey and Speer, 1985; Speer and Aubrey, 1985]. The mutual interference of an astronomical tide and a shallow water tide can give rise to tidal asymmetry [Kang and Jun, 2003]. To study the tidal asymmetry in these estuaries, the simulations of observed tides during March–April 2003 were carried out. Thereafter, the harmonic analysis of observed and simulated tides was carried out. Tidal constituents derived from harmonic analysis were analysed to study the nonlinear response of the Mandovi and Zuari estuarine system to tidal forcing.

3.3.1 Simulation of tides measured during March–April 2003

The model was run for 42 days (3 March–13 April 2003) to simulate tides at 13 stations in the Mandovi and Zuari estuaries. Even in April, there is a small fresh water influx ($10\text{--}15\text{ m}^3\text{ s}^{-1}$) into the Mandovi and Zuari estuaries from the upstream ends; hence river discharge of $10\text{ m}^3\text{ s}^{-1}$ was introduced at the upstream end boundaries in the Mandovi and Zuari estuaries. The model was spun up over a period of 7 days (3–9 March 2003) and the simulated tides of the remaining days (10 March–13 April 2003) were compared with those observed. The observed and simulated tides at 13 stations in the main channels

of the Mandovi and Zuari and in the Cumbarjua are plotted in Figures 3.11– 3.13. The model has reproduced the tidal observations reasonably well in almost all the stations. Verem station in the Mandovi is about 5 *km* from the mouth where tide is about 1.5 and 2.3 *m* during neap and spring tide respectively. Tidal ranges remain almost the same at Britona (9 *km*), Akkada (20 *km*), Volvoi (33 *km*) and Usgao (41 *km*) with slight increase in amplitude toward the upstream regions. But when tide reaches Ganjem (50 *km*), the tidal oscillation is visible only during spring tide. Similarly, tides at Dona Paula (0 *km*), Cortalim (12 *km*), Borim (21 *km*) and Sanvordem (45 *km*) also remain unchanged, but the magnitude of tide gets distorted at Sanguem (55 *km*). The simulation of tides at Banastarim (15 *km*) and Madkai (24.5 *km*) in the Cumbarjua are also well reproduced by the model.

3.3.2 Harmonic analysis of tides

The purpose of harmonic analysis of tide is to find out the amplitude and phase of each individual constituents from a long tidal record (1 month or more) so that each constituent's role on the tidal distortion in an estuary can be studied in detail. In the present study, Tidal Analysis Software Kit-2000 was used for harmonic analysis of tides. The 35-day data of observed and simulated tides were used for harmonic analysis, and this 1-month's duration of data was sufficient to resolve the major diurnal and semidiurnal constituents; overtides and compound tides.

3.3.3 Complex difference module

To find the difference between observed and simulated tidal constituents, the complex difference module was computed. The complex difference module gives synthetic information about the difference in both amplitude and phase between the observation and simulation. The mean difference of this module over major diurnal and semidiurnal con-

Figure 3.11 Observed (dotted line) and simulated (solid line) tides in the Mandovi estuary during 10 March–13 April 2003. 144 *hours* on the x-axis correspond to 0.0 *hours* (IST) on 10 March 2003.

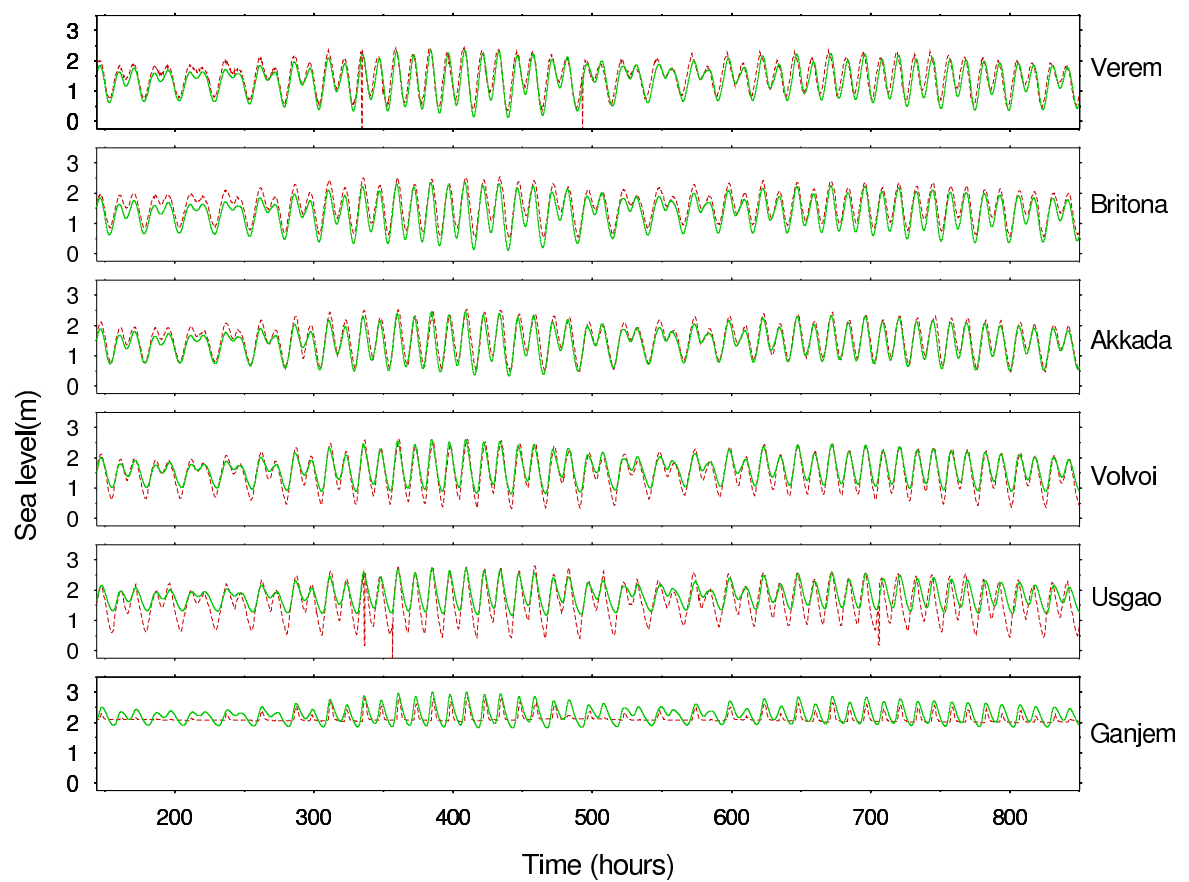


Figure 3.12 Observed (dotted line) and simulated (solid line) tides in the Zuari estuary during 10 March–13 April 2003. 144 *hours* on the x-axis correspond to 0.0 *hours* (IST) on 10 March 2003.

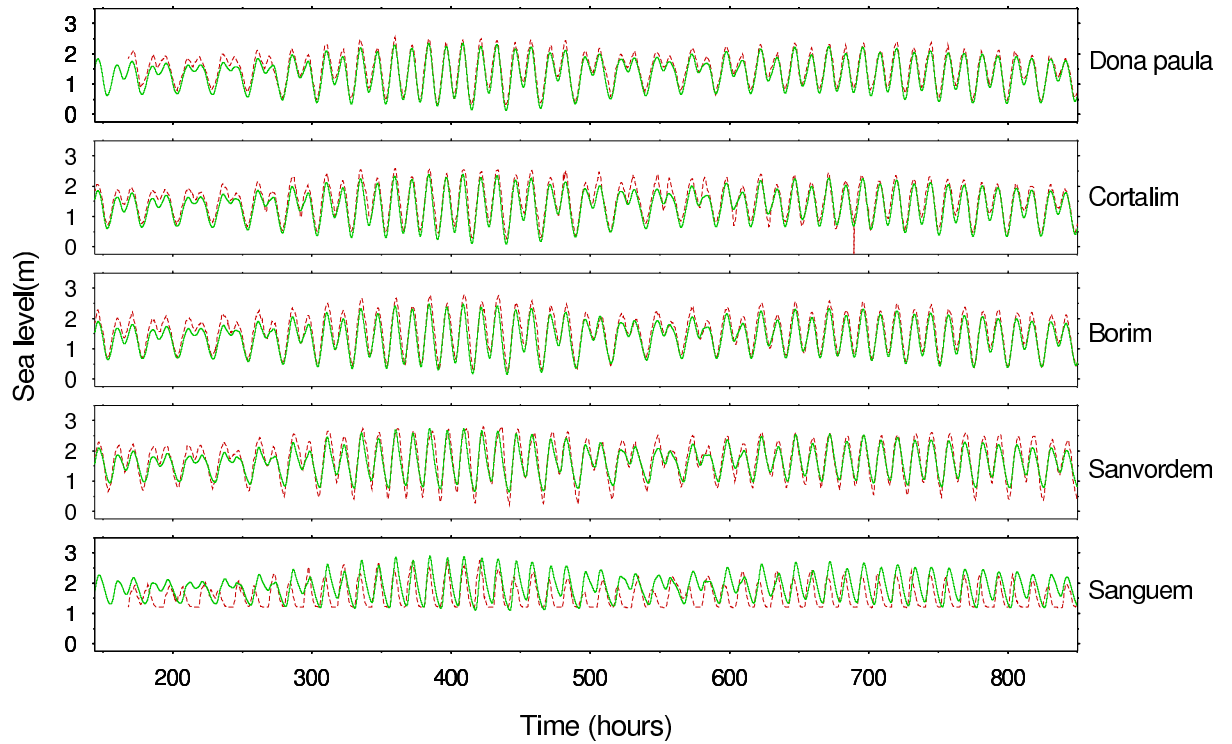
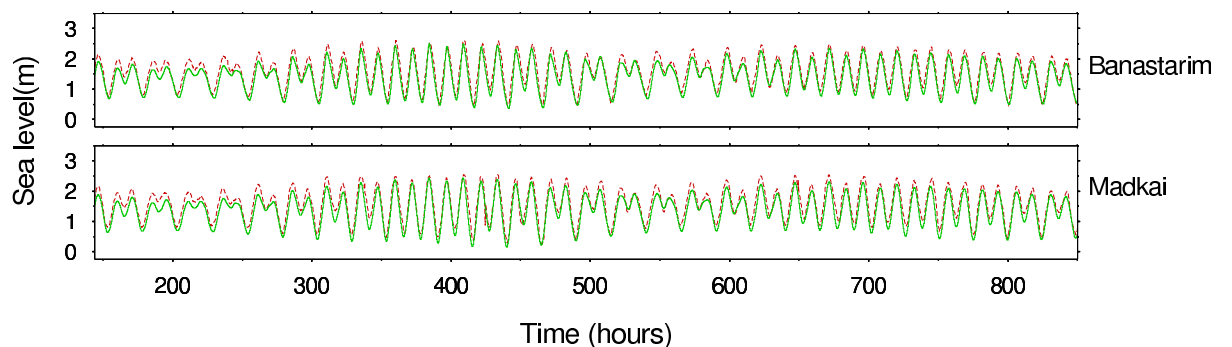


Figure 3.13 Observed (dotted line) and simulated (solid line) tides in the Cumbarjua canal during 10 March–13 April 2003. 144 *hours* on the x-axis correspond to 0.0 *hours* (IST) on 10 March 2003.



stituents, over tides and compound tides was also calculated to get the mean estimate of the accuracy of the model at each station. The amplitudes and phases of observed and simulated tidal constituents and the complex difference module are given in Tables 3.1 – 3.3. The five major diurnal and semidiurnal constituents in Tables 3.1 and 3.2 are plotted in Figure 3.14. Overtides and compound tides are shown in Figures 3.15 and 3.16 respectively. As discussed earlier, M_2 is the dominant tidal constituent with amplitude of more than 50 *cm* both in the Mandovi and Zuari estuaries. The other dominant constituents are K_1 , S_2 , O_1 and N_2 (see Tables 3.1 and 3.2).

Table 3.1 Amplitudes (Amp), Phases (Pha) and Complex difference module (Diff) of tidal constituents in the Mandovi estuary. The number in bracket shown for each station name is the distance (*km*) from the mouth of the estuary.

Constituents (<i>cm</i>)	Verem[5]			Britona [9]			Akkada [20]			Volvoi [33]			Usgao[41]			Ganjem [50]			
		Obs	Model	Diff	Obs	Model	Diff	Obs	Model	Diff	Obs	Model	Diff	Obs	Model	Diff	Obs	Model	Diff
O_1	Amp	14.9	17	2.6	14.7	17	2.4	14.5	16.4	1.9	14.3	14.7	1.7	15	13.5	1.9	2.3	12.5	13.36
	<i>Pha</i>	51.2	57.1		54.7	57.8		60.8	62.7		62.7	69.6		67.1	71.9		327.9	75.1	
K_1	Amp	35.5	32.5	4.5	33.7	32.6	2	34.1	32.2	2.11	33.5	31.3	5.4	36.6	30.5	7.09	6.1	28.6	22.64
	<i>Pha</i>	61.5	69.2		67	69.9		75	76.6		77.5	86.3		83.2	89.4		82.1	93	
N_2	Amp	12.3	12.4	1.8	12.4	12.5	4.3	12.8	12.3	5.3	14.3	12.1	3.7	15.8	12.1	5.3	2.8	11.6	8.8
	<i>Pha</i>	299.5	291		312.3	292.4		329.1	304.8		336.3	323.2		345.1	329		333.9	335	
M_2	Amp	53.2	54.2	1.7	52.4	54.4	10.88	55.3	54.2	14.33	61.1	55.1	7.9	63.6	55.6	10	12.1	53.9	42.71
	<i>Pha</i>	318.2	316.7		329.6	318.1		345.5	330.5		353.3	348.2		0	354.2		20.92	1.1	
S_2	Amp	18.2	20.8	3	17.4	20.9	4.19	17.9	20.4	5.5	19.6	20.1	1.4	20.6	20.3	2.6	5.7	19.7	4
	<i>Pha</i>	358.1	2.8		11.1	4.2		32.5	17.5		41.3	37.4		51	43.5		48.9	49.9	
mean diff of major constituents				2.7			4.7			5.8			4			5.4			18.3
M_4	Amp	0.6	1.3	0.7	1.5	1.3	0.9	1.2	0.5	1.5	1.7	2.8	2.5	2.3	4.3	2.1	6.4	6.1	10
	<i>Pha</i>	25.1	18.1		72.2	24.5		284.8	359		199.2	261.6		237.2	267.2		35	287.4	
M_6	Amp	0.4	0.8	0.6	0.6	0.8	0.4	0.9	0.9	1.0	1.9	1.1	1.4	2.2	1.1	1.4	2.6	1.2	1.8
	<i>Pha</i>	301	251		292.5	255.5		5	291.1		44	352.2		67.5	33.7		44.5	84.2	
mean diff of overtides				0.6			0.7			1.2			2			1.7			5.9
MSf	Amp	4.3	3.6	2.3	4.5	3.6	2.8	4.8	3.4	1.4	5	4.1	0.9	4.8	4.7	1.4	4.1	5.4	1.9
	<i>Pha</i>	342.1	309.1		349	309.2		329.8	326		5.1	0.4		354.3	11.9		40	22.6	
MK_3	Amp	0.7	1.4	1.7	0.3	1.4	1.3	1	2	1.3	2.2	3.5	2.15	2.3	4.3	2	3	4.9	4.7
	<i>Pha</i>	245.5	350.6		279.9	351.3		326.9	1.8		329.1	5.1		12.7	9.4		86.8	17.9	
MN_4	Amp	0.5	0.5	0.06	0.7	0.5	0.5	0.1	0.2	0.2	0.8	1.2	1.0	1.7	2.0	1	2.5	2.8	3.8
	<i>Pha</i>	25.1	18.1		72.2	24.5		284.8	359		199.2	261.6		237.2	267.2		12.55	279.8	
MS_4	Amp	0.5	1.7	2.1	0.8	1.7	2.2	0.6	2.1	2.4	1.8	3.8	3.3	2.5	5.1	2.6	5.8	6.5	6.3
	<i>Pha</i>	166	10.2		132.6	12.1		253.4	12.6		292.9	354.4		344.1	355.1		63.31	1.4	
mean diff of compound tides				1.5			1.7			1.3			1.8			1.7			4.2

Table 3.2 Amplitudes (Amp), Phases (Pha) and Complex difference module (Diff) of tidal constituents in the Zuari estuary. The number in bracket shown for each station name is the distance (*km*) from the mouth of the estuary.

Constituents (<i>cm</i>)	Dona Paula [0]			Cortalim [12]			Borim [21]			Sanvordem [45]			Sanguem [55]			
		Obs	Model	Diff	Obs	Model	Diff	Obs	Model	Diff	Obs	Model	Diff	Obs	Model	Diff
O_1	Amp	16.9	17	0.44	14.7	17.1	2.78	13.9	16.7	3.72	16.2	15.4	1.43	7.6	9.7	14.86
	<i>Pha</i>	55.6	57.04		62.6	57.5		52.1	61.3		62.9	67.2		190.6	72.7	
K_1	Amp	32.4	32.4	0.7	35.5	32.7	4.9	38.8	32.8	6.7	37.4	32.2	5.9	17.9	22.9	37
	<i>Pha</i>	67.7	69.1		63.1	70		70	74.9		78.3	82.9		220.9	90.6	
N_2	Amp	12.4	12.4	0.6	12.3	12.8	0.5	15.8	13.1	4.7	13.9	14	5.1	12.1	9.9	4.2
	<i>Pha</i>	288.1	290.9		292.3	292.5		318	302.2		339.3	317.9		308.5	327.6	
M_2	Amp	54	53.9	2.1	59.9	55.9	4.3	63.8	57.7	10	69.7	62.6	11.36	42.6	44.5	29.9
	<i>Pha</i>	313.7	316		319.6	318		335	327.4		350.1	342.4		317.2	357.3	
S_2	Amp	20.7	20.7	1	19.8	21.5	1.7	21.6	21.9	2.7	22.9	23.5	7.1	13.6	17.1	14.9
	<i>Pha</i>	359.7	2.6		3.1	4.4		22	14.7		48.8	31.2		345.9	42.8	
Mean diff of major constituents				1			2.8			5.6			6.2			20.2
M_4	Amp	1.2	1.2	0.1	2.7	1.4	2.2	3.6	1.0	2.6	4.9	5.2	5.3	6.3	5.1	2.0
	<i>Pha</i>	40.8	46		117.1	62.5		140.6	131		157.3	221		251	267.9	
M_6	Amp	0.7	0.7	0.1	0.4	1	0.6	0.8	1.1	0.7	1.8	1.7	0.1	1.7	1.3	1.2
	<i>Pha</i>	242.4	250.6		284	256		327.9	283.6		44.3	42.5		63.3	108.9	
Mean diff of overtides				0.1			1.4			1.6			2.7			1.6
MSf	Amp	3.6	3.6	0	2.3	3.6	2.5	5.1	3.5	3.2	4.2	4.1	1.5	10.3	5.1	5.4
	<i>Pha</i>	308.9	308.9		354	310.1		2.4	323.7		15.7	354.3		16.3	28.9	
MK_3	Amp	1.4	1.4	0.11	0.8	1.5	1.2	1.2	1.9	2.3	3.6	3.7	2.6	5.2	3.4	7.3
	<i>Pha</i>	346.3	351		47.4	348		250.3	348.5		305.8	348.8		133.2	16.8	
MN_4	Amp	0.5	0.5	0.05	1.2	0.5	0.9	1.4	0.3	1.1	2.4	1.9	2.5	3.9	2.3	1.6
	<i>Pha</i>	11.3	16.4		77.7	34.7		135.7	107.7		144.7	215		258.3	266	
MS_4	Amp	1.7	1.7	0.1	0.5	1.7	2	2.1	1.5	3.5	4.5	4.4	5.8	4.2	5.4	5.1
	<i>Pha</i>	3.9	9.6		136.8	12.3		198	0		244.3	326.8		283.8	347.7	
Mean diff of compound tides				0.08			1.6			2.5			3.1			4.9

Table 3.3 Amplitudes (Amp), Phases (Pha) and Complex difference module (Diff) of tidal constituents in the Cumbarjua canal. The number in bracket shown for each station name is the distance (*km*) from the mouth of the estuary.

Constituents (<i>cm</i>)		Madkai [15]			Banastarim [24.5]		
		Obs	Model	Diff	Obs	Model	Diff
O_1	Amp	14.3	15.9	3.7	14.1	16.7	5.4
	<i>Pha</i>	56.4	69.4		42.6	60.5	
K_1	Amp	34.5	32.7	7.7	34.8	32.6	2.2
	<i>Pha</i>	72	84.8		73.5	73.7	
N_2	Amp	13.3	11.8	1.7	14.4	12.8	1.6
	<i>Pha</i>	322.4	318		298.5	299.7	
M_2	Amp	55.7	54.8	2.3	57.6	56.3	1.3
	<i>Pha</i>	340.4	342.7		325.4	325.1	
S_2	Amp	18.4	19.9	2.2	19.6	21.4	2.1
	<i>Pha</i>	26.4	31.2		15.4	12	
mean diff of major constituents				3.57			2.5
M_4	Amp	2	3	4.7	0.5	1	0.7
	<i>Pha</i>	116.9	257.9		149.6	101.2	
M_6	Amp	1.5	0.8	0.7	0.3	1.1	0.8
	<i>Pha</i>	318.2	308.7		270.6	274.2	
Mean diff of overtides				2.7			0.7
MSf	Amp	5	3.6	2.8	6.5	3.5	3.5
	<i>Pha</i>	3.2	328.9		343	321.3	
MK_3	Amp	0.9	3.7	3.2	1.8	1.7	3
	<i>Pha</i>	295.8	351		228.3	349.7	
MN_4	Amp	0.8	1.2	1.9	0.2	0.3	0.1
	<i>Pha</i>	99.3	259.2		47.6	73.5	
MS_4	Amp	1	3.8	4.4	0.5	1.4	1.9
	<i>Pha</i>	210.1	336		193.9	8.6	
Mean diff of compound tides				3.1			2.1

3.3.4 Major diurnal and semidiurnal constituents

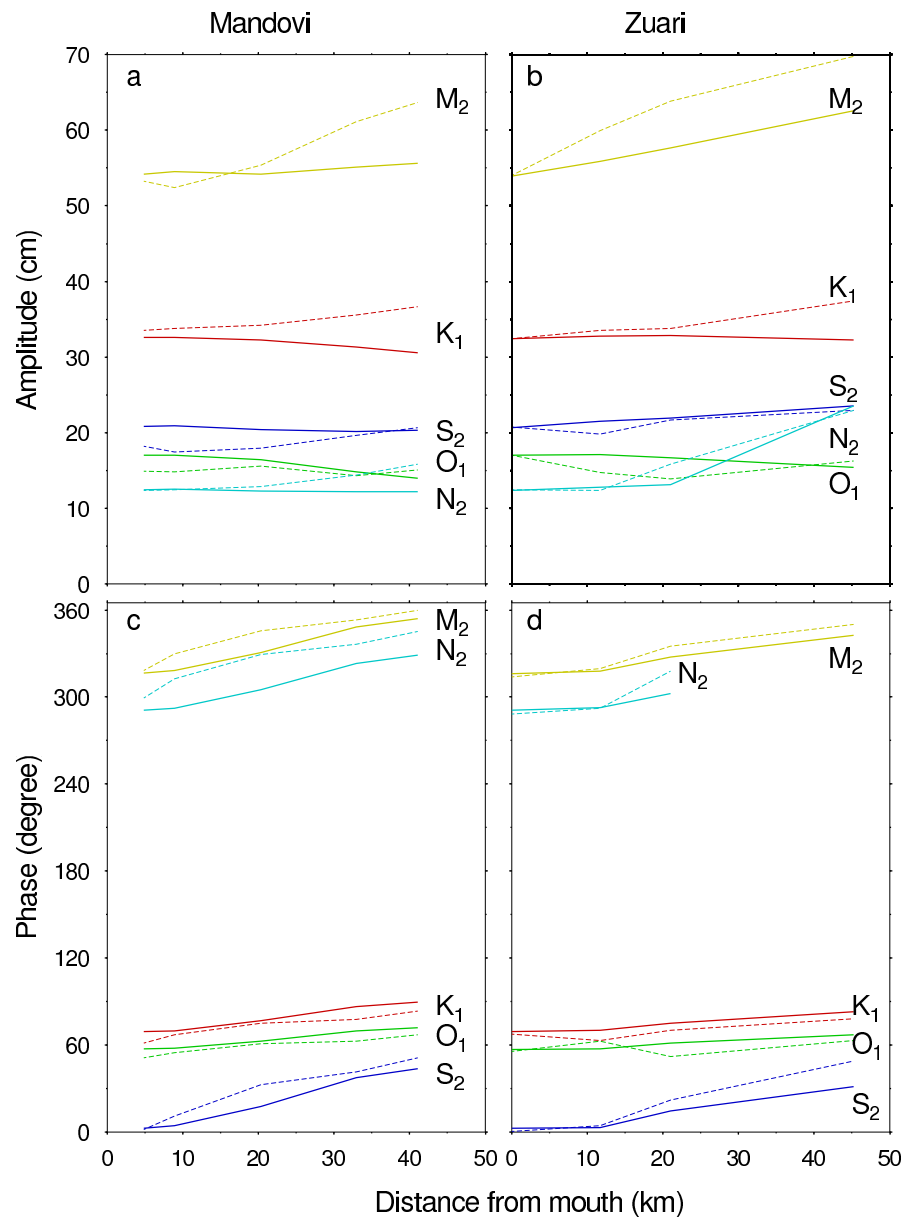
Figure 3.14 shows the observed and simulated amplitudes and phases of five major tidal constituents. The observed amplitude of M_2 in the Mandovi is 53 *cm* at Verem and the amplitude increases to about 63 *cm* at Usgao. Thus, the increase of M_2 tide when it reaches the upstream regions is about 10 *cm*. In the Zuari, the amplitude of M_2 is about 54 *cm* at Dona Paula, and the amplitude increases to about 69 *cm* at Sanvordem. Amplitudes of K_1 , S_2 , O_1 and N_2 also increase toward the upstream regions. Now if we look at the simulations of these constituents, at Verem, Britona and Akkada, the simulation

of the amplitude of M_2 is reasonably good, but at Volvoi and Usgao, the model underestimates M_2 . In the Zuari, the model reproduces M_2 reasonably well from Dona Paula to Sanvordem (see Figure 3.14b). The simulation of the amplitudes of O_1 , N_2 and S_2 are also reasonably good in both the Mandovi and Zuari. The model underestimates the amplitude of K_1 at upstream regions, but the model has reproduced the phase increase of diurnal and semidiurnal constituents toward the upstream regions reasonably well both in the Mandovi and Zuari. The mean difference of major constituents at different stations except Ganjem and Sanguem in the Mandovi and Zuari are within the limits of model accuracy (see Tables 3.1 and 3.2). The differences found at Ganjem and Sanguem are very high, and the reasons are explained in the Discussion section.

3.3.5 Overtides and compound tides

Overtides are plotted in Figure 3.15, which show the longitudinal variation of amplitude and phase of M_4 and M_6 toward the upstream regions. The simulations of overtides are reasonably good in the Mandovi and Zuari. Both observation and simulation show the rapid increase of M_4 inside the Zuari. The amplitude and phase of M_6 , which is the second harmonic of M_2 , also increases inside these estuaries. The amplitude of M_6 is better simulated than M_4 in both these estuaries. Figure 3.16 shows that MSf (lunisolar synodic fortnightly constituent) is a significant compound tidal constituent in the Mandovi and Zuari with its amplitude of about 3 cm (see Tables 3.1 and 3.2) at the downstream regions and increases about 5 cm at the upstream regions. Two other important compound tides are MK_3 (ter-diurnal tide, derived from the interactions of M_2 and K_1) and MN_4 (quarter-diurnal tide which is the result of M_2 and N_2 interactions). The amplitude and phase of MK_3 steadily increase inside these estuaries. The simulations of the amplitude and phase of MN_4 is well matched with that observed in the Mandovi and there is a reasonably good match in the Zuari. The simulation of the amplitude of MS_4 (quarter-diurnal compound tide which is the result of M_2 and S_2 interactions) also has a reasonable

Figure 3.14 Variation in amplitude (*cm*) and phase (*degree*) of observed (dotted line) and simulated (solid line) five major tidal diurnal and semidiurnal constituents in the Mandovi and Zuari estuaries.



match in the Zuari, but the model overestimates the amplitude in the Mandovi. The mean difference of overtides and compound tides increases marginally from mouth to upstream stations.

3.3.6 M_4/M_2 amplitude ratio and relative surface phase ($2M_2 - M_4$)

M_4/M_2 amplitude ratio and relative surface phase ($2M_2 - M_4$) help to determine the nonlinear distortion of tides inside the estuaries. Relative phasing of M_4 to M_2 determines whether an estuary is flood dominant or ebb dominant [Aubrey and Speer, 1985; Speer and Aubrey, 1985; Friedrichs and Aubrey, 1988]. M_4/M_2 is almost steady in the Mandovi estuary (see Table 3.4) and it steadily increases in the Zuari from the mouth to upstream regions. The model overestimates M_4/M_2 at the upstream regions in the Mandovi, and the simulation of M_4/M_2 overall is good in the Zuari (see Table 3.5). The relative surface phase decreases toward the upstream regions in both the Mandovi and Zuari estuaries.

Table 3.4 M_4/M_2 amplitude ratio and relative surface phase ($2M_2 - M_4$) in the Mandovi estuary

	Verem[5]		Britona [9]		Akkada [20]		Volvoi [33]		Usgao[41]		Ganjam [50]	
	Obs	Model	Obs	Model	Obs	Model	Obs	Model	Obs	Model	Obs	Model
M_4/M_2	0.01	0.02	0.03	0.02	0.02	0.009	0.02	0.04	0.03	0.07	0.52	0.11
$2M_2 - M_4$ (degree)	222.3	226	207.7	222.5	172.7	259.6	145.6	68.2	100.1	73.6	6.8	74.8

Table 3.5 M_4/M_2 amplitude ratio and relative surface phase ($2M_2 - M_4$) in the Zuari estuary

	Dona Paula [0]		Cortalim [12]		Borim [21]		Sanvordem [45]		Sanguem [55]	
	Obs	Model	Obs	Model	Obs	Model	Obs	Model	Obs	Model
M_4/M_2	0.02	0.02	0.04	0.02	0.05	0.01	0.07	0.08	0.14	0.11
$2M_2 - M_4$ (degree)	222.6	226	162.1	213.5	169.4	163.4	182.9	103.7	23.4	86.7

Figure 3.15 Variation in amplitude (*cm*) and phase (*degree*) of observed (dotted line) and simulated (solid line) overtides in the Mandovi and Zuari estuaries.

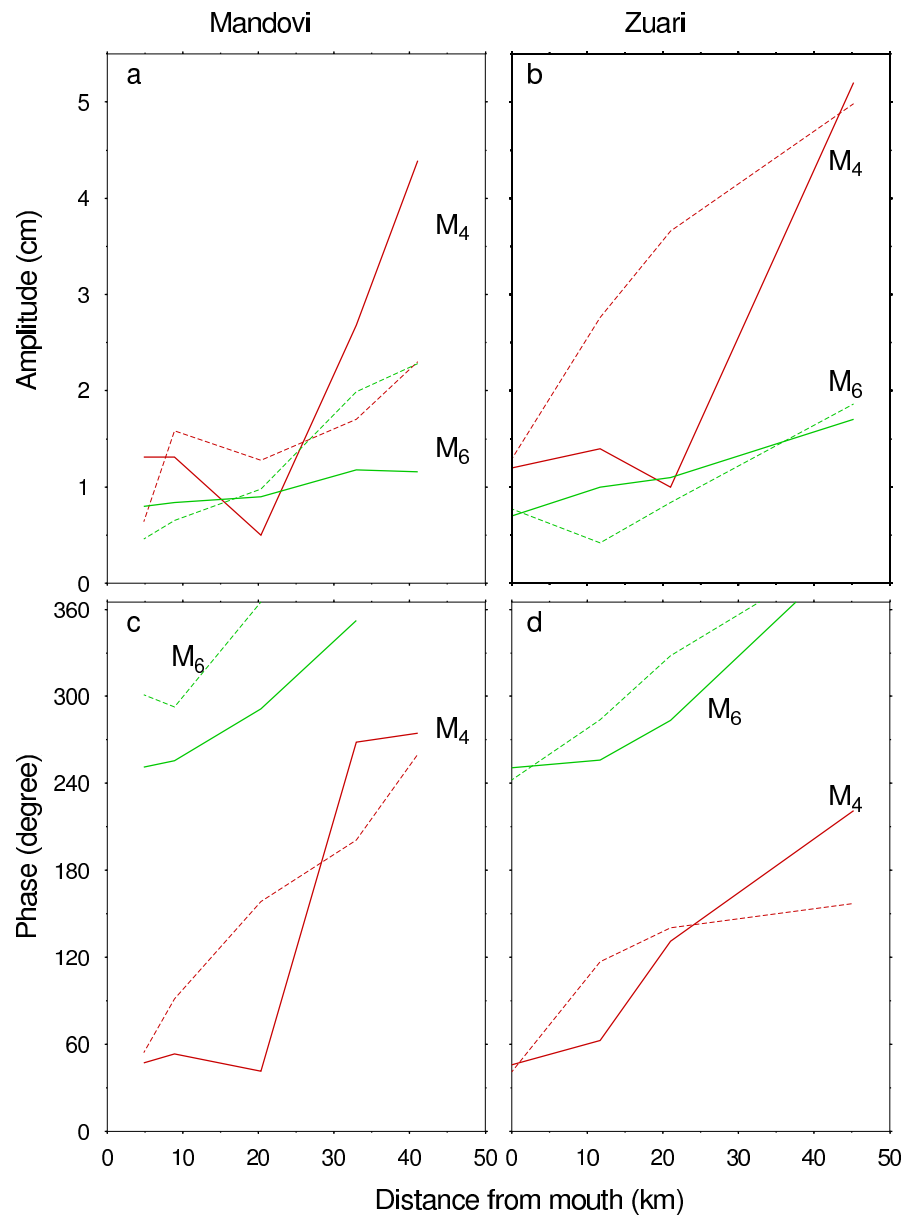
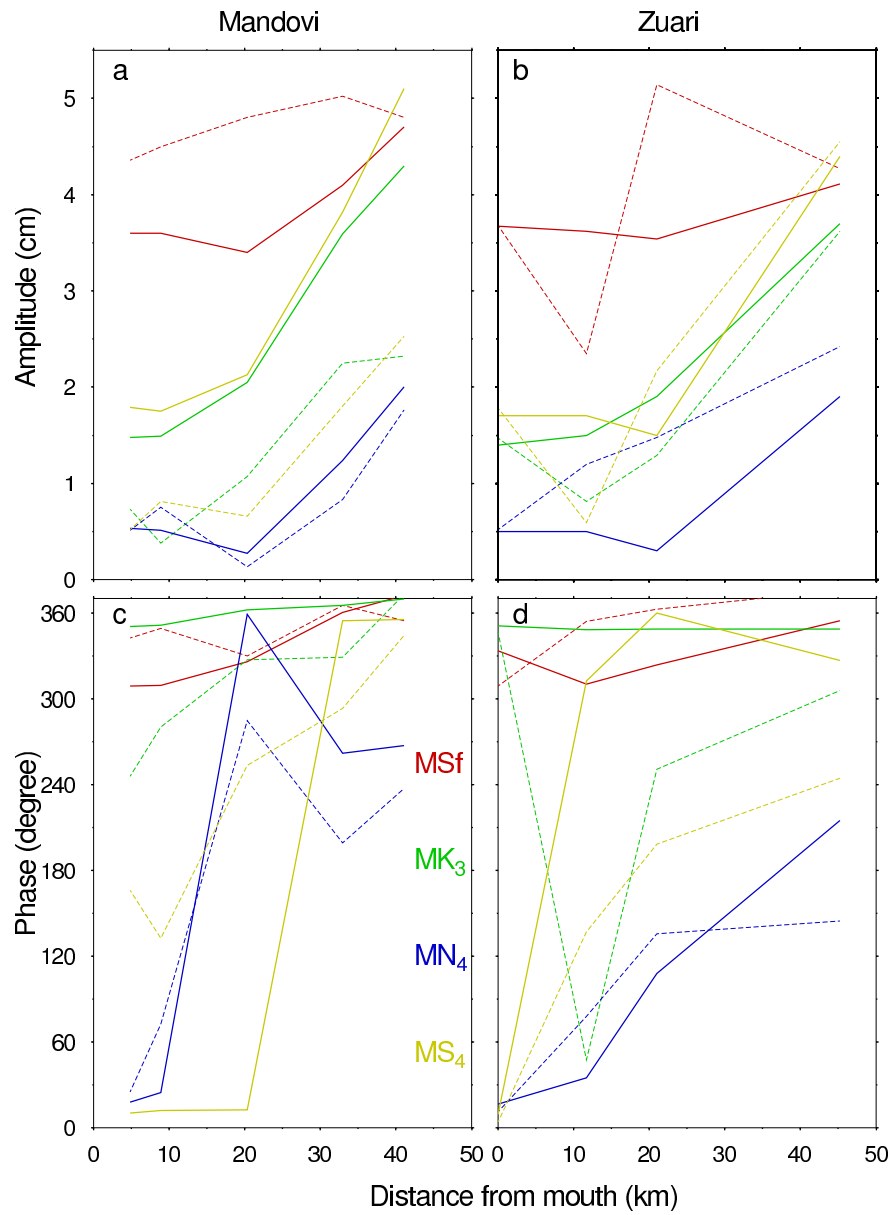


Figure 3.16 Variation in amplitude (*cm*) and phase (*degree*) of observed (dotted line) and simulated (solid line) compound tides in the Mandovi and Zuari estuaries.



3.4 Discussion

The present study describes tidal circulation in the Mandovi and Zuari estuaries. The study also focuses on the freshwater influence on tides and tidal asymmetries. The model sensitivity to horizontal diffusion of momentum was checked and the coefficient value was allowed to vary between 100 and 700 m^2s^{-1} . The increase in amplitude and phase of tidal constituents toward the upstream regions was better simulated for the value of 500 m^2s^{-1} . The changes in friction from 0.001 to 0.003 did not show any significant impact on amplitude and phase, however the value, 0.002 showed better agreement between the observed and simulated tides.

3.4.1 Longitudinal variation in tidal amplitudes

Tidal amplitudes in the Mandovi and Zuari estuaries slightly increase toward the upstream regions (Figures 3.1 – 3.4). This is due to the rapid decrease in channel's width toward the upstream regions. Ganjem is located at the upstream end of the Mandovi estuary (Figure 3.1c) where the tidal range is about 0.5 m during dry season. This indicates that even a small volume of river discharge through a narrow channel is sufficient to prevent tide entering the upstream regions. The channel's elevation from the sea level is also a factor preventing the tidal propagation further toward upstream regions, but at Sanguem (Figure 3.2 c), the tidal amplitude is not decayed much. This is due to two factors (i) the volume of the river runoff in the Zuari is smaller than compared to Mandovi during dry season, and (ii) the width of the channel is larger than that of the Mandovi. During wet season, the tidal oscillations are minimum at these two stations because of heavy fresh water influx (300–500 m^3s^{-1}). This was confirmed by the model results when fresh water influx of 400 m^3s^{-1} was introduced at upstream boundaries in the Mandovi and Zuari. Tidal amplitude in the Cumbarjua canal (Figures 3.2 b and 3.3 b) is almost similar to that of Zuari. This could be due to the fact that the cross sectional area of the Cumbarjua

canal at the junction with the Zuari is larger than that of the Mandovi. So tide propagates into the Cumbarjua canal freely from the Zuari.

3.4.2 Tidal currents and mixing of water column

One of the main purposes of using a 2D and 1D coupled model was to simulate tidal currents in the down stream regions in the Mandovi and Zuari estuaries. Fairly strong tidal currents and the absence of river discharge mixes the water column vertically during the dry season in these estuaries. During wet season, the velocity associated with river discharge prevents upstream propagation of tides [Unnikrishnan et al., 1997]. The tidal influence is very low at the upstream regions during wet season and the saline water gets pushed toward the mouth of these estuaries.

3.4.3 Nonlinearity in tidal propagation in the Mandovi and Zuari estuaries

Tidal observations in March–April 2003 show that the tidal amplitude remains almost same with slight increase in the upstream direction in the Mandovi and Zuari estuaries over a long stretch. The previous studies in the Mandovi and Zuari estuaries show that tidal amplitude remains unchanged over a distance of 40 *km* from the mouth and then decays rapidly over the next 10 *km* [Shetye et al., 1995; Unnikrishnan et al., 1997]. The Mandovi and Zuari estuaries are strongly converging channels and this leads to the amplification of tides in the upstream direction. The momentum balance in this type of estuary is primarily between pressure gradient and friction [Friedrichs and Aubrey, 1994], the decay in amplitude due to friction gets cancelled by geometric amplification, which leaves the amplitude, unchanged over 40 *km* in the Mandovi and Zuari estuaries from the mouth. Tidal amplitude gets decayed in the remaining 10 *km* in these estuaries. Unnikrishnan et al. [1997] showed that the decay in amplitude at the upstream regions was because of

the influence of river discharge. The influence of river discharge is visible even in April at Ganjem.

3.4.4 Increase in amplitudes and phases of major constituents

Harmonic analysis of tides shows that the predominant species of tidal constituents increase inside these estuaries (see Figure 3.14). As we have seen, the Mandovi and Zuari estuaries are not frictionally dominated estuaries; the frictional nature of the estuary is demonstrated by the significant decay of all semidiurnal and diurnal constituents, with associated large phases [Aubrey and Speer, 1985]. The previous studies [Unnikrishnan et al., 1999a; Shetye, 1999; Unnikrishnan and Luick, 2003] show that major diurnal and semidiurnal constituents increase inside the Gulf of Khambhat and Gulf of Kutch because of quarter wave length resonance and geometric effects. Shetye [1999] showed that the large amplification in semidiurnal constituents in the Gulf of Kutch is due to the proximity of their periods to the period at which the gulf resonates. Though we have not estimated the role of co-oscillation of incident and reflected waves in amplitude and phase in the Mandovi and Zuari estuaries, it can be seen from Figures 3.15 and 3.16 that the amplitude and phase variations of the tidal constituents toward the upstream regions are not linear, which is a strong indication of the presence of a reflected wave in these estuaries. Hence the amplification of semidiurnal constituents in the Mandovi and Zuari can be mainly attributed to the balance between pressure gradient and friction as mentioned previously. The superimposition of incident and reflected wave could be the other cause for the increase in semidiurnal constituents in the upstream directions.

3.4.5 Increase in amplitude and phase of overtides and compound tides

Nonlinear response to the tidal forcing is reflected in the increase of high frequency M_2 over tide, compound tides and a forced low frequency MSf constituent throughout the estuary [Aubrey and Speer, 1985]. The increase of M_4 toward the upstream regions in an estuary indicates flood dominance. M_4 increases both in the Mandovi and Zuari estuaries. Similarly, amplitude and phase of M_6 increase inside the estuaries. Increase of M_6 inside the estuaries can be attributed to the quadratic friction [Blanton et al., 2002]. The nonlinear increase of compound tides toward the upstream regions can be seen in Figure 3.16. Both observation and simulation show a consistent increase of amplitude of MSf in the Mandovi though the model slightly underestimates amplitude in the downstream regions, but the observed amplitude increase of MSf inside the Zuari is not consistent. The amplitude of MN_4 in the Mandovi and MS_4 in the Zuari decreases in the middle regions of these estuaries and then steadily increase to the upstream directions. This rapid increase in amplitude and phase of the first and second harmonics of M_2 and the nonlinear increase of compound tides show the nonlinear nature of the Mandovi and Zuari estuarine systems to the tidal forcing.

The complex difference module calculated at different stations in the Mandovi and Zuari shows that the mean differences over major diurnal and semidiurnal constituents, overtides, and compound tides gradually increase from the downstream region to the upstream regions. The difference in M_2 is also high toward the upstream stations. For the present study, a 2D square grid was used, which is not well adapted to the irregular configuration of coastlines. The meandering effects of channels influence the amplitude and phase of tide entering into the estuary. The higher difference found in some stations between observed and simulated could be due to these reasons. Now, if we look at the difference calculated at Ganjem and Sanguem, the differences are very high between observed and simulated tidal constituents. Apart from the above cited reasons, there are

other factors such as river discharge, and higher channel elevation with respect to mean sea level, which also prevent tide from entering these upstream stations. River discharge into the Mandovi is more than that of the Zuari. Thus, the tidal characteristics get distorted more at Ganjem than at Sanguem. Tide is visible at Ganjem only during spring tide. Hence the harmonic analysis of tidal signal measured at Ganjem did not resolve the amplitude and phase of tidal constituents accurately.

The increase of M_4/M_2 amplitude ratio toward the upstream regions is marginal, except Ganjem in the Mandovi estuary, (see Table 3.4) the M_4/M_2 is 0.01 at Verem and 0.03 at Usgao. This increase of M_4/M_2 from the mouth to upstream regions shows that tides do not get distorted much toward the upstream regions in the Mandovi whereas at Ganjem, tide gets completely distorted as it is evident from the very high amplitude ratio, which is about 0.5. In the Zuari, tidal amplitude gets distorted toward the upstream regions with the continuous increase of M_4/M_2 from 0.02 to 0.1 (see Table 3.5). The observations of relative surface phase decrease from 222° at Verem to 6.8° at Ganjem in the Mandovi. In the Zuari, the observation of relative surface phase decrease from Dona Paula to Cortalim, but from Cortalim to Sanvordem, the relative surface phase increases and again it decreases at Sanguem (see Tables 3.4 and 3.5). But the model shows a decrease in relative surface phase toward the upstream directions both in the Mandovi and Zuari with exceptions at Akkada and Usgao. Now if we look at the relative phase relationship between M_4 and M_2 , a flood-dominant system has a sea surface phase of 0° to 180° with maximum flood at 90° and ebb-dominant system has sea surface phase of 180° to 360° with maximum ebb at 270° [Friedrichs and Aubrey, 1988]. If we assume a linear relationship in the relative phase mentioned previously, a relative surface phase of about 220° at Verem and Dona Paula, and about 6° at Ganjem, and about 23° at Sanguem show that the relative surface phase decreases toward the upstream regions. The decrease of a relative surface phase toward upstream directions is an indication of flood-dominance. Analysis of sea level observations (see Figure 3.11 and 3.12) also show the flood-dominance in the

Mandovi and Zuari estuaries. Overall, the increase of M_4 and decrease of relative surface phase in both the Mandovi and Zuari show that these estuaries are flood-dominated. But there are some mudflats at the upstream regions in the Zuari estuary, that can increase the duration of ebb, which indicates that the Zuari estuary is less flood-dominant than the Mandovi estuary.

3.5 Conclusion

The study shows that tides in the Mandovi and Zuari estuaries undergo longitudinal variation due to geometry of channels, channel elevation with respect to the mean sea level and also due to river discharge from the upstream regions. The hybrid network model used for the study reproduced tides and showed freshwater influence on tides. Harmonic analysis of the observed and simulated tides was carried out to study the nonlinear nature of tidal propagation in the Mandovi and Zuari estuaries. The observations and model results show the consistent increase of amplitude and phases of major diurnal and semidiurnal constituents inside these estuaries. The increase of amplitudes and phases of major tidal constituents inside the estuaries show that the Mandovi and Zuari estuaries are not frictionally dominated estuaries because the frictional effect is balanced by the geometric effect. The increase of overtides and compound tides inside the estuaries show the nonlinearity of these estuaries to tidal forcing. The M_4/M_2 amplitude ratio shows that tidal distortion in the upstream regions in the Mandovi is marginal, whereas in the Zuari, the M_4/M_2 amplitude ratio steadily increases in the upstream direction. This higher amplitude ratio indicates strong tidal distortion in the Zuari.